Int. J. Electrochem. Sci., 10 **(2015)** 9751 - 9765

International Journal of
ELECTROCHEMICAL
SCIENCE
www.electrochemsci.org

DFT Calculations, Electrical and Thermal Properties of Unsubstituted Triphenylformazan

O. E. Sherif

Chemistry Department, Faculty of Science, Cairo University, Giza, Egypt, 12613.
E-mail: oe_sherif@hotmail.com

Received: 20 June 2015 / *Accepted:* 11 September 2015 / *Published:* 30 September 2015

Unsubstituted triphenylformazan (TPF) is prepared by the common method. This molecule possesses two possible forms, cyclic and open structures. Quantum-chemical calculations of both cyclic and open structures indicate that the cyclic structure involves predominantly the intramolecular hydrogen bonding. Moreover, this form is the one responsible for the experimental measured conductance and electrical properties of TPF. The dependence of dielectric and electrical properties of unsubstituded triphyenylformazan (TPF) on temperature from 300-400 K and the frequency from 0.1-20 KHz was studied. The dielectric constant ε' is directly proportional to temperature and has indirect relationship with frequency. The same trend was observed for the dielectric loss ε". The thermal analyses concerning thermagravimentric analysis (TGA), differential thermal analysis (DTA) and differential scanning calorimetry (DSC) were also performed. The DC conductivity in two temperature regions was studied. At lower temperature region the DC conductivity increases while at higher temperature region the conductivity decreases with the temperature increase. This behaviour was correlated to the change in hydrogen bonding. Based on the experimental results concerning AC conductivity and the frequency exponent (s) the charge transport mechanism is best illustrated through the correlated barrier hopping (CBH) model. The electrical conduction may be protonic.

Keywords: formazan, DFT calculations, electrical properties, thermal studies, conduction mechanism

1. INTRODUCTION

Formazans are class of organic compounds which are colored owing to π- bonds and contain the characteristic chain of atoms –N=N–C=N–NH– attached to aromatic or non-aromatic groups. A large number of formazans has been prepared and a study for structures was carried out [1-6].

TPF can exist in two forms depending on the temperature: cyclic requires a hydrogen bond between H29 and N3 and open structures. There is also the possibility that the open form can exist in the cis- and trans- configurations via rotation around N2–N3.

Some organic compounds are utilized as semiconductors. Said semiconductors can be used instead of the usual inorganic semiconductor technology. Rogers and Ubbelohde [7] assumed that hydrogen bonding causes proton conduction in solids [8,9,10].

As many studies have been carried out on formazans [11-12] a few number discussed the electrical properties and DFT calculations [11,13].

In the present work, the structural studies of unsubstituted triphenylformazan were characterized. The dielectric properties, DC and AC conduction mechanisms are discussed. The correlation of thermal properties of unsubstituted triphenylformazan (TGA, DTA and DSC) with its structure is studied.

The molecular structure of the investigated formazan may be represented by the following formula:

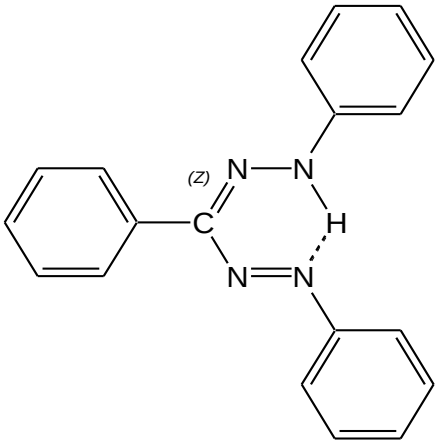

In order to support the experimental findings, quantum-chemical calculations at the Density Functional Theory (DFT) level is carried out for the two possible structures of TPF, which are the open structure, capable of forming intermolecular hydrogen bonding and the cyclic structure, capable of forming intramolecular hydrogen bonding, as shown in Figure 1.

2. EXPERIMENTAL

1,3,5-triphenylformazan was synthesized by adding gradually the appropriate diazonium salt solution (0.005 mol), which was prepared by the known procedure from aniline, to benzaldehyde phenylhydrazone (0.005 mol) dissolved in sodium hydroxide solution with constant stirring [3,6]. The prepared mixture was kept overnight in refrigerator, then hydrochloric acid (1:1) is added to the cold solution. The obtained product was separated by filtration then being washed with water and crystallized (from ethanol) to constant melting point [mp 173-174 ˚C, (lit. 172-174 ˚C) [3]]. The formazan was also subjected to elemental analysis.

In order to measure the electrical properties, a disk of the prepared material was pressed of thickness ~ 0.1cm as previously described [9].

Shimadzu-50 thermal analyzer (Japan) was used to perform thermal analysis starting from ambient temperature to 700^{o}C at a heating rate 10^{o}C per minute using Al_2O_3 as a reference material in case of DTA and DSC. Quantum-chemical calculations of TPF carried out at B3LYP/6-31G* level for open and cyclic structures, shown in Figure 1 using Gaussian 09 package [14].

3. RESULTS AND DISCUSSION

3.1. Quantum-chemical Calculations

TFP can exist either as open or cyclic structure. In the open structure, there is a possibility that it can exist as a cis- or trans- conformer by rotating about N2-N3 bond, as shown in Figure 1. Optimized geometry (the global minimum for *trans-syn-s-cis*) conformation is carried out for the open form and for the cyclic form where the energies of both forms are found to be the same. On the other hand, the open structure can be involved in intermolecular hydrogen bonding formation between N3 of one molecule and H29 of the other molecule. However this trial to get the optimized structure has failed because of the excessive bond distance (~6 Å), as shown in Figure 2.

Reference to the previous findings, it was found that the intramolecular hydrogen bonding between N3 and H29 in the same molecule is the dominant hydrogen bonding, as shown in Figure 1. Tazcan and Tokay [11] used PBE1PBE functional with 6-311G (2d,2p) basis set for geometry optimization of TPF [11]. It was shown that the amount of cyclic structure was greater than that of open structure.

The results of quantum-chemical calculations of the possible open and cyclic structures, shown in Figure 1, are listed in Table 1.

It is obvious, from the table analysis, that the two forms have nearly the same energy, atomic charges and bond lengths values. It is clear that there is no H29-N3 bond exists for the open structure. Dipole moment of the cyclic structure is calculated to be 2.52 D, while that of the open structure is 2.26 D indicating higher dipole of the former over the latter implying that the intramolecular hydrogen bonded-structure is the one responsible for the electrical properties shown by the experimental findings. This verifies that the protonic conduction via the charged hydrogen bonded structure is the mechanism responsible for the conduction. The comparison of the electron density contours of HOMO of cyclic and open structures shows noticeable difference of electron distribution of both forms, where the cyclic structure electron density is higher than that of the open structure, as shown in Figure 3, indicating that the cyclic (intramolecular hydrogen bonded form) is the form responsible for protonic electric conductance.

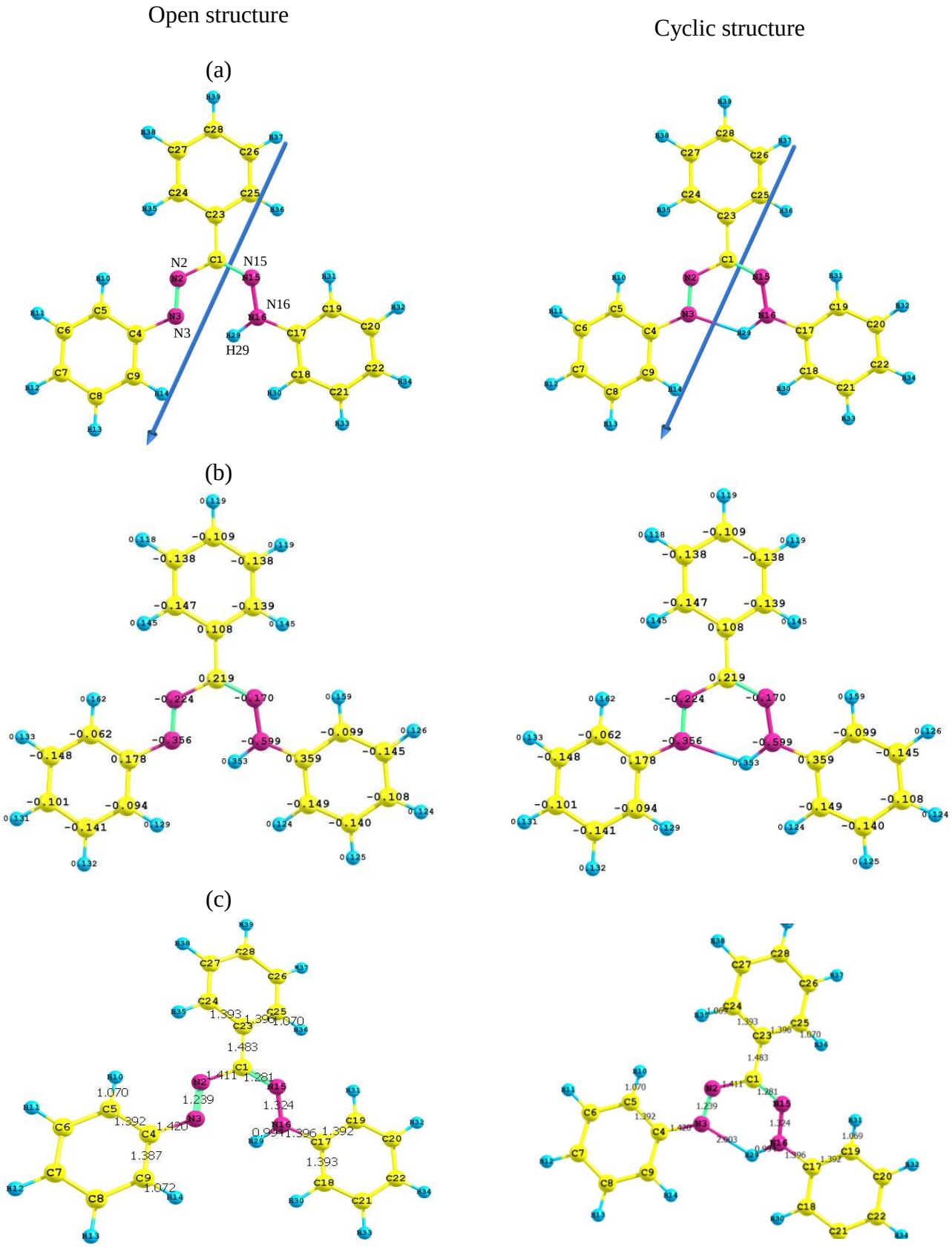

Figure 1. (a)The optimized geometry and vector of the dipole moment (b) net charges and (c) bond lengths of the open and cyclic structures using B3LYP/6-31G*

Before optimization After optimization

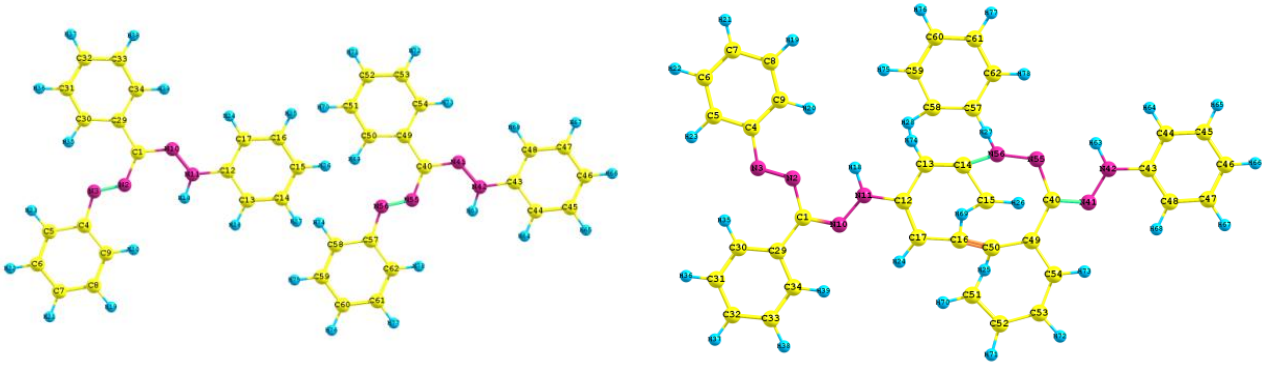

Figure 2. Structure of the intermolecular hydrogen bond in TPF.

Table 1. Total energy, energy of HOMO and LUMO, dipole moment, atomic charges and bond lengths for cyclic and open structures of TPF using B3LYP/6-31G*.

Parameter	Cyclic	Open
E_T, au	-952.3404	-952.3404
E_{HOMO}, au	-0.1977	-0.1974
μ, D	2.5236	2.2659
Atomic charges		
N2	-0.224	-0.224
Cl	0.219	0.219
N15	-0.17	-0.17
N16	-0.599	-0.599
H29	0.356	0.356
N3	-0.356	-0.356
Bond lengths, Å		
Cl—N15	1.281	1.281
N15—N16	1.324	1.324
N16—H29	0.99	0.99
H29—N3	2.003	
N3—N2	1.239	1.239
N2—Cl	1.411	1.411

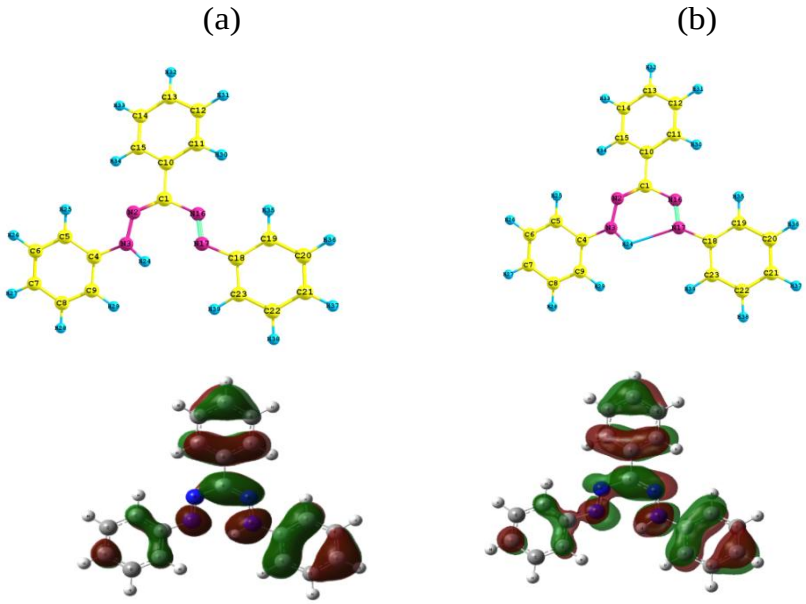

Figure 3. The HOMO charge density maps of (a) open and (b) cyclic forms of TPF using B3LY/6-31G*

3.2. Direct current (DC) electrical conductivity

The electrical conductivity as a function of temperature was studied in two temperature regions. The first region lies at T < 357 K. At this region as the temperature increases the conductivity increases. This may be explained on the basis that in this region, the sample has semiconducting properties [15], and the activation energy decreases. In the second region T > 357 K the conductivity decreases with increasing temperature, as shown in Figure 4. Activation energy-temperature dependence follows the Arrhenius relation:

$$\sigma = \sigma_0 \exp(-E_a/KT) \quad (1)$$

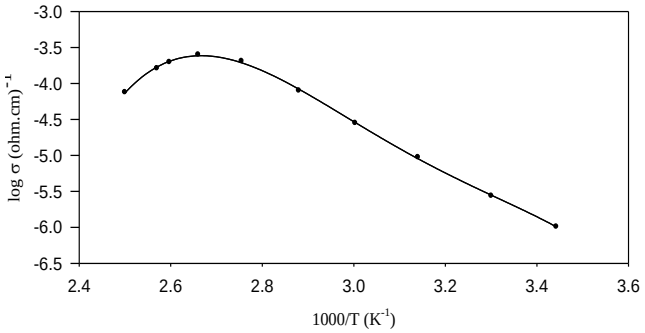

Figure 4. Variation of the DC conductivity with temperature

E_a is the activation energy of charge-transfer and K is Boltzmann constant. The activation energy values vary with the change in structure of the compound [16]. The relation between logσ and temperature shows two regions. This means that the activation energy was changed on passing from one region to the other. The explanation of this change may be due conformational and/or the conduction mechanism changes. In the previous investigation [6] of unsubstituted triphenylformazan, it was pointed out that TPF is found to be in its intramolecular NH…N=N hydrogen bonded azo-hydrazo-tautomeric form [11, 17]. This finding is confirmed by the quantum-chemical calculation as mentioned before.

The mechanism of conduction in compounds containing hydrogen bonds may be protonic [8]. In this mechanism the conduction takes place in terms of the movement of protons through the localized system. In the light of this proposal the low temperature conduction may be protonic. π-electrons delocalization plays an important role in the hydrogen bond strength [18,19].

It was stated that intramolecular hydrogen bond is inversely changed with temperature. As the temperature increases, the intramolecular hydrogen bond weakened resulting in the increase of the localization of π-electrons and hence, the conductivity decreases.

3.3. Dielectric permittivity

It was concluded that there is a direct proportional relation between temperature and dielectric constant ε', while indirect proportional between ε' and frequency meaning that ε' increases as temperature increases whereas it decreases as frequency increases [20-21]. Said findings of the dielectric constant were conducted at frequency range 0.1-20 KHz and temperature range 300-400 K as illustrated in Figures 5, 6.

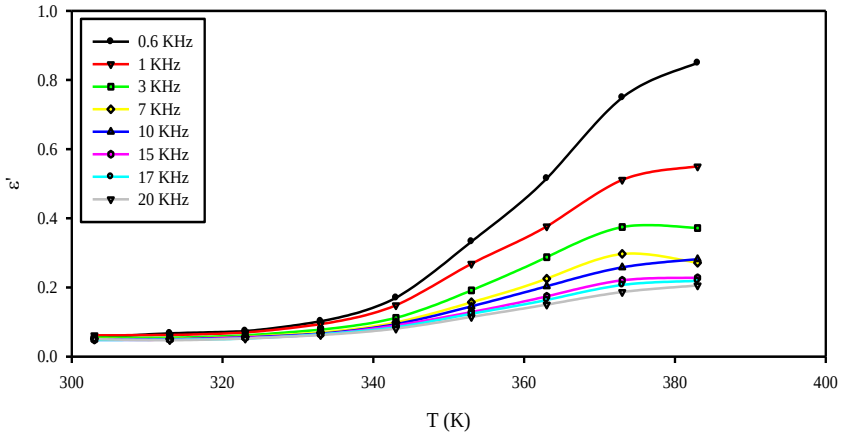

Figure 5. Change of the dielectric constant ε' relative to temperature at different frequencies

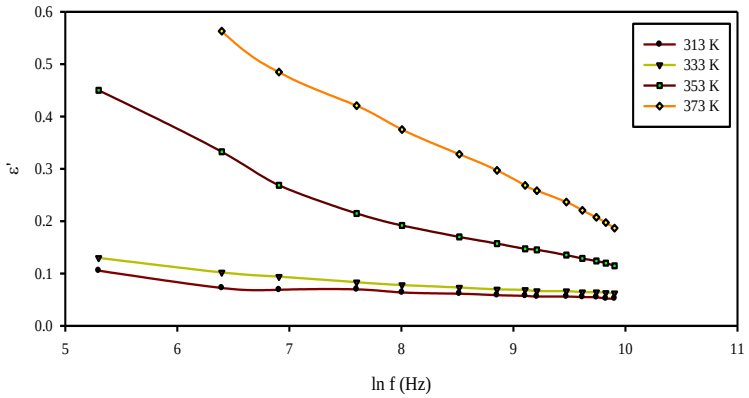

Figure 6. Variation of the dielectric constant ε' with frequency at different temperatures

Taking into consideration the dependence of ε' on temperature variation, it was obvious that if the charge carriers are not in the direction of the field, their contribution to the polarization is weak and this affects the change of ε' with temperature. Hence, the increase in temperature results in sufficient thermal excitation energy obtained by the bound charge carriers which enhances the polarization leading to the increase in the dielectric constant ε' [22].

On the contrary ε' decreases as frequency increases, which may be due to the inability of the dipoles to rotate fastly so, they oscillate behined the field. Same trend as dielectric constant goes with dielectric loss ε" noting that at given frequency, dielectric loss increases with the temperature increase given that at T $\geq$ 350 K while at lower temperature T < 350 K, the change is small. It is worth mentioning that the relation between ε" and temperature is realized at low frequency meaning that ε" increases with temperature if the value of f $\leq$ 1 KHz as being illustrated in Figure 7.

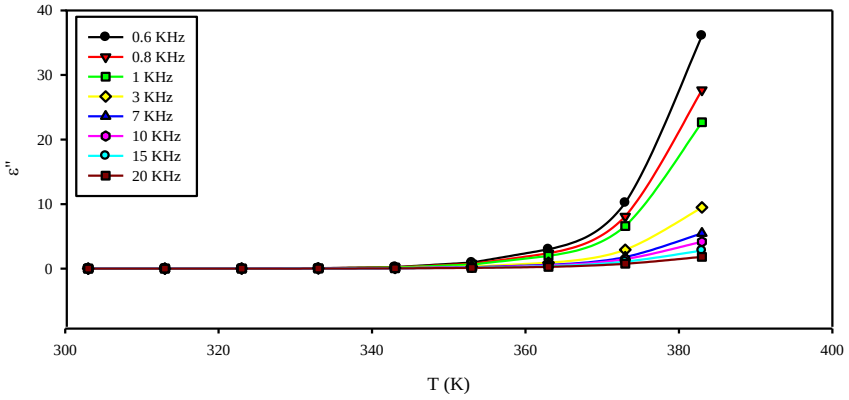

Figure 7. Temperature dependence of the dielectric loss ε" at different frequencies

The relation between ε" and frequency at different temperatures explains the behaviour of dielectric loss with temperature and frequency. Referring to Figure 8, it is apparent the negative correlation between ε" and frequency showing that at different temperatures a series of straight lines

with different slopes are formed reflecting that as the temperature increases consequently, ε" increases while frequency decreases.

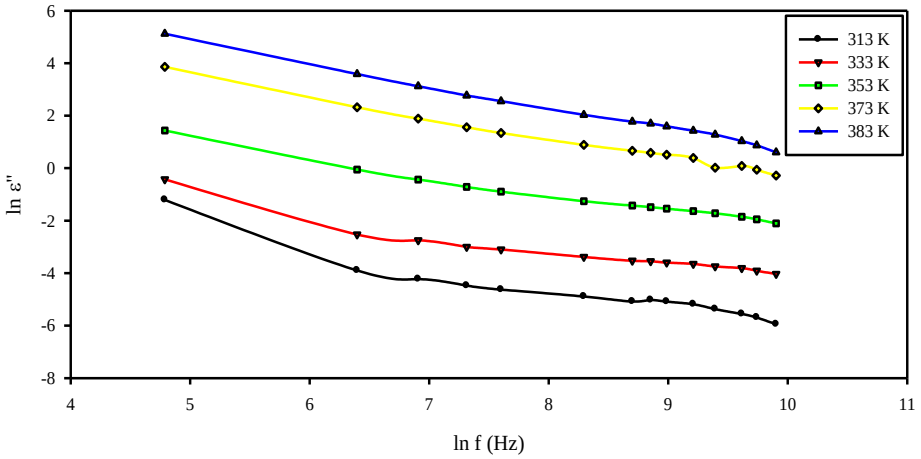

Figure 8. Frequency dependence of the dielectric loss **ε** " at different temperatures

The relation between ε" and frequency goes through the following equation:

$$\varepsilon'' = (\varepsilon_s - \varepsilon_\infty)\, 2\pi^2\, N\, (ne^2/\varepsilon_s)\, K\, T\, \tau_0^m\, W_m^{-4}\, \omega^m \qquad (2)$$

In which

ε_s: the static dielectric constant,

ε_∞: the dielectric constant at infinite frequency.

N: the density of localized states at which carriers exist

n: the number of polarons involved in the charge transfer process.

W_m: the barrier height and,

ω: the angular frequency, τ_0 is the characteristic relaxation time.

According to the proposed theory, the frequency dependence of ε" should follow the power law:

$$\varepsilon'' = G\, \omega m \qquad (3)$$

Where G is a pre-exponential factor and ω is the angular frequency.

3.4. The relation of alternating current (AC) conductivity towards to the change in temperature and frequency

The total conductivity σ_{total} (ω) is explained as per the following equation [23].

$$\sigma_{total}(\omega) = \sigma_{ac}(\omega) + \sigma_{dc} \qquad (4)$$

where σ_{ac} (ω) is the AC conductivity and σ_{dc} is the DC conductivity.

The above equation is used when AC and DC are obtained through separate mechanisms while in the limit ω → (0) [24] AC conductivity is similar to DC conductivity.

3.5. Temperature dependence

The effect of temperature and frequency on the alternating current conductivity is shown in Figure 9. which represents the change in conductivity as a function of $\frac{1}{T}$ in the temperature range 300 – 400 K at different frequencies. From the figure it can be shown that the conductivity slightly changes till 310 K then the conductivity increases with increase in temperature. This behaviour may be explained on the basis that the increase in temperature affects the hydrogen bond strength in the molecules. From Figure 9. it is apparent that the alternating current conductivity increases with increasing the frequency at given temperature.

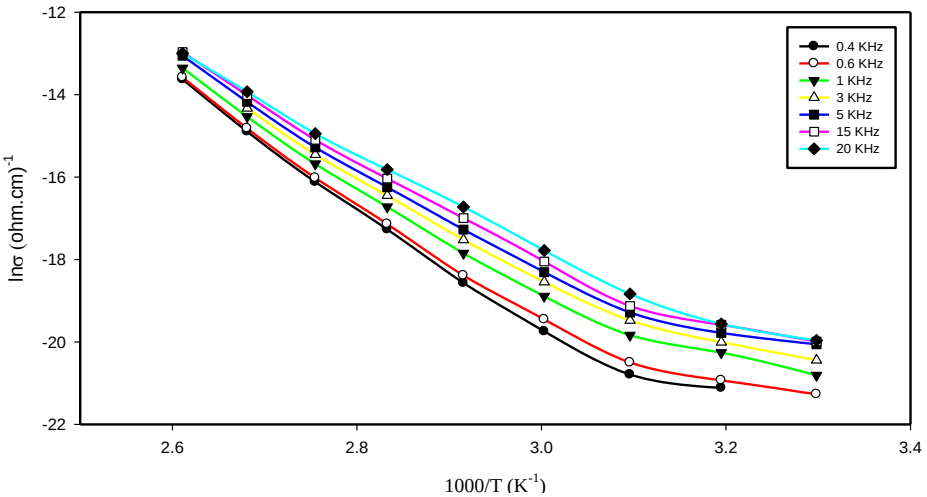

Figure 9. Variation of the AC conductivity with temperature at different frequencies

From the relation of ln σ_{ac} and lnf represenled in Figure 10, it is evident that the alternating current conductivity increases as the frequency increases at certain temperature. This indicates that the hopping of charge carriers between the localized states is improved as the frequency increases. Accordingly, it is evident that the mechanism of conduction could be due to hopping [25, 26].

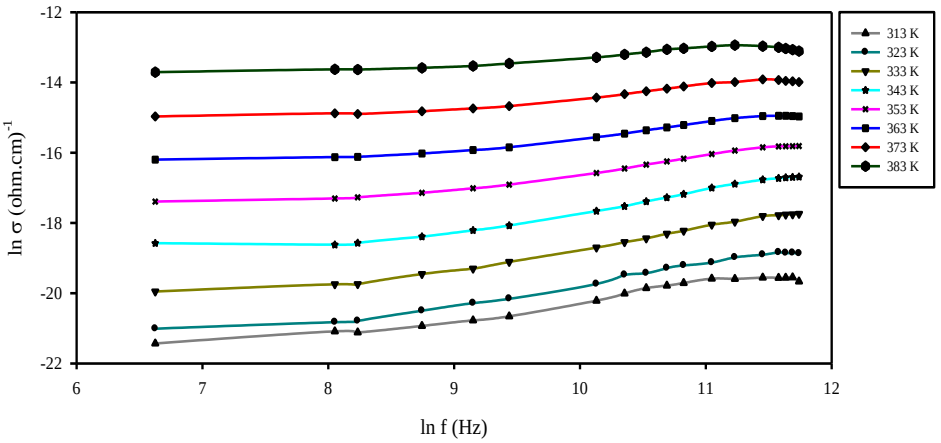

Figure 10. The relation between AC conductivity and frequency at various temperatures

The slope of each linear part, in Figure 10, gives the exponent (s) at that temperature. The relation between the exponent (s) and temperature is represented in Figure 11. Referring to this figure, it is clear that as the temperature increases the exponent (s) decreases. The hopping mechanism is considered since log σ_{ac} is dependent on frequency [25, 26].

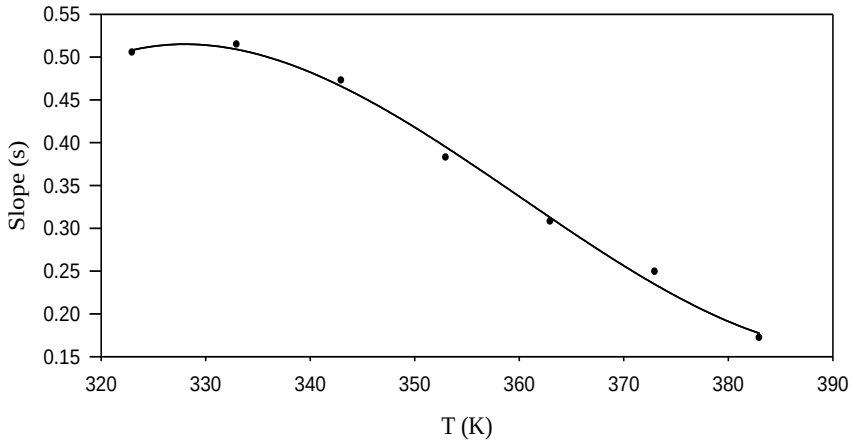

Figure 11. Temperature dependence of the exponent (s)

The conduction mechanism of alternating current conductivity can be suggested from the behaviour of (s) [27-29], which may be occurred through two different types of mechanisms; the first one known as quantum mechanical tunneling (QMT) [30, 31] and the second one is classical hopping over a barrier (HOB) [23, 32]. In the first model the frequency exponent (s) does not change with change of temperature but dependent of frequency variation with a value of 0.81 [24]. From Figure 11, it is evident that with the temperature increase the value of (s) decreases in contrast with the quantum mechanical model. So, for the formazan under investigation this model is not the most suitable one to illustrate the charge transport mechanism. On the other hand, the value of (s) equal to unity for the second model "classical hopping over a barrier" [32], while the experimental calculated value of (s) is 0.5 indicating that this model is not applicable for the studied TPF to explain the mechanism of conduction.

Another suggested model is the correlated barrier hopping (CBH). Pike [33] and Elliot [26] developed the (CBH) model for single– and two– electrons, respectively. In this model the relation between the relaxation variable, W, and R, the intersite separation, is established. The columbic reaction from W_m to W, represented by the relation:

$$W = W_m – (ne^2 / \pi \varepsilon_1 \varepsilon_0 R) \quad (5)$$

In which: ε_0: the dielectric permittivity of free space

ε_1: the dielectric constant of the material

Other symbols are previously explained.

The equation shows the relation between the frequency exponent and temperature [23, 24, 34] is shown as:

$$s = 1\text{-}6\ Kt / [W_m + KT \ln (\omega\tau_0)] \quad (6)$$

where, τ_0 is the characteristic relaxation time which is of the order of an atomic vibrational period.

In conclusion, as per the CBH model, it was shown that with the increase in temperature, there is decrease in the exponent (s). Said results are not compatible with the QMT or simple HOB mechanisms. Hence, in the analysis of the investigated formazan, the conduction mechanism is best illustrated by using the CBH model.

3.6. Thermal parameters

a) The thermogravimetric analysis (TGA) plot

Referring to Figure 12, in critical temperature region "300-400 K", there was no weight loss, however, a weight change took place within range 400-873 K as a result of decomposition of TPF.

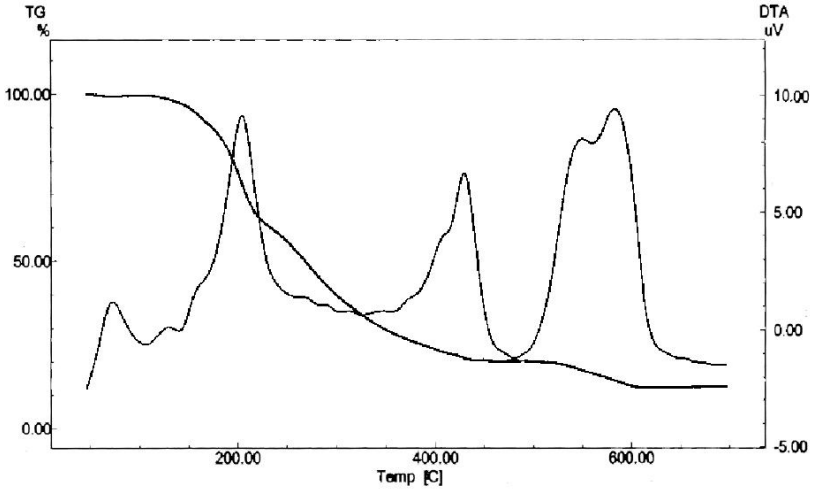

Figure 12. TGA and DTA thermograms for TPT

b) Differential thermal analysis (DTA)

DTA thermogram for the formazan (TPF) is shown in Figure 12. The scanning rate was 10 ˚C min^{-1}. The presence of the endothermic peak at 380 K is due to dehydration of hygroscopic water. It is observed that the decomposition of TPF occurs in three steps which are represented by the exothermic peaks in the DTA curve.

c) Differential scanning calorimetry (DSC)

As illustrated in Figure 13, at 10 ^oC min^{-1} heating rate, there are two endothermic peaks were evidenced through the DSC thermogram. The first peak was shown at $\simeq$ 315 K being a result of dehydration, the other peak was noticed at $\simeq$ 467 K from melting [35, 36].

The most important characteristic resulting from the DTA and/or DSC thermogram is that there is no structural change in the investigated temperature region. This confirms that the electrical parameters with temperature are not of structural phase transition.

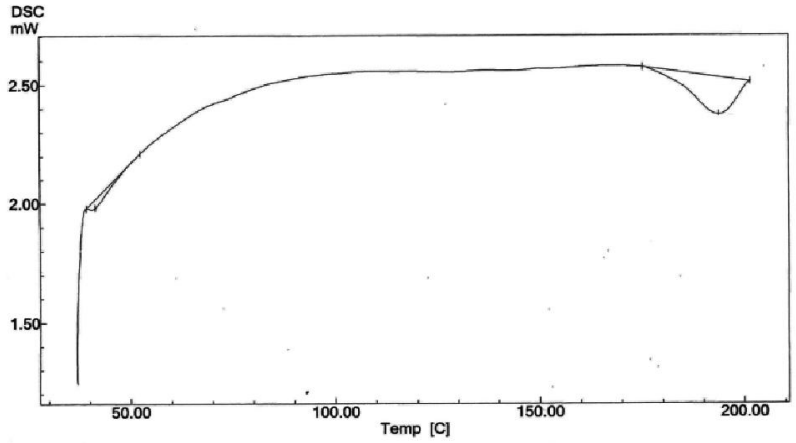

Figure 13. DSC plot for TPF

4. CONCLUSIONS

Quantum-chemical calculations of unsubstituted triphenylformazan show that the open and cyclic structures differ in dipole moment which suggests that the cyclic intramolecular hydrogen bond form is dominant over the open structure accounting for the protonic conduction. Said results are considered compatible to the expected examined findings.

Unsubstituted triphenylformazan exists predominantly in the cyclic form as it is evident from the magnitude of its dipole moment and electron charge distribution verifying the possibility of a proton transfer process which is expected to lead to protonic conduction since, hydrogen bonding is a pre-requisite for such conduction. Our study discussed and examined the DC and AC electrical conductivities, dielectric constant and dielectric loss of 1,3,5–triphenylformazan. The DC electrical conductivity indicates semiconductor behavior. Based on our study, it is evidenced that the dielectric constant and dielectric loss have a direct proportional relationship with temperature while being indirectly related to frequency (i.e ε' and ε" increase as frequency decreases).

The electric conduction seems to be protonic in addition of the possibility of electron conductivity where the transport of protons and delocalization of π-electrons are the main cause of the electrical conduction. In conclusion the correlated barrier hopping (CBH) model is the suitable model for conduction mechanism in TPF under study. Finally, according to TGA, DTA and DSC results no phase transition up to 400 K took place.

ACKNOWLEDGEMENT
I would like to express my deep thanks for Prof. Dr. Afaf Abdel Razik, Professor of Inorganic Chemistry, Chemistry Department, Faculty of Science, Cairo University for her kind advice and valuable help.

References

1. J. W. Lewis and C. Sandorfy, *Can. J. Chem.*, 61 (1983) 809.
2. A. R. Katritzky, S. A. Belyakov, D. Cheng and H. D. Durst, *Synthesis*, 5 (1995) 577.
3. H. Tezcan and N. Ozkan, *Dyes and Pigments*, 56 (2003) 159.
4. N. T. Abdel-Ghani, Y. M. Issa and O. E. Sherif, *Thermochim. Acta*, 138 (1989) 129.
5. O. E. Sherif, Y. M. Issa, M. E. Hassouna and S. M. Abbas, *Monatsh. Chem.*, 124 (1993) 627.
6. N. T. Abdel-Ghani and Z. Z. Sharara, *Egypt. J. Chem.*, 32 (1989) 533.
7. S. E. Rogers and A. R. Ubbelohde, *Trans. Faraday Soc.*, 46 (1950) 1051.
8. M. M. Abdel-Kader, F. El-Kabbany, H. Naguib and W. M. Gamal, *Phase Transitions*, 81 (1) (2008), 83.
9. H. Hassib and A. Abdel Razik, *Solid State Comm*., 147 (2008), 345.
10. T. Anfimova, Q. Li, J. O. Jensen and N. J. Bjerrum, *Int. J. Electrochem. Sci.*, 9 (2014) 2285.
11. H. Tezcan and N. Tokay, *Spectrochem. Acta*, 75 (2010) 54.
12. H. Tezcan and E. Uzluk, *Dyes Pigments*, 75 (2007) 633.
13. G. Turkoglu, H. Berber and I. Kani, *New J. Chem.*, 39 (2015), 2728.
14. M. J. Frisch; G. W. Trucks; H. B. Schlegel; G. E. Scuseria; M. A. Robb; J. R. Cheeseman; G. Scalmani; V. Barone; B. Mennucci; G. A. Petersson; H. Nakatsuji; M. Caricato; X. Li; H. P. Hratchian; A. F. Izmaylov; J. Bloino; G. Zheng; J. L. Sonnenberg; M. Hada; M. Ehara; K. Toyota; R. Fukuda; J. Hasegawa; M. Ishida; T. Nakajima; Y. Honda; O. Kitao; H. Nakai; T. Vreven; J. A. Montgomery Jr.; J. E. Peralta; F. Ogliaro; M. Bearpark; J. J. Heyd; E. Brothers; K. N. Kudin; V. N. Staroverov; R. Kobayashi; J. Normand; K. Raghavachari; A. Rendell; J. C. Burant; S. S. Iyengar; J. Tomasi; M. Cossi; N. Rega; J. M. Millam; M. Klene; J. E. Knox; J. B. Cross; V. Bakken; C. Adamo; J. Jaramillo; R. Gomperts; R. E. Stratmann; O. Yazyev; A. J. Austin; R. Cammi; C. Pomelli; J. W. Ochterski; R. L. Martin; K. Morokuma; V. G. Zakrzewski; G. A. Voth; P. Salvador; J. J. Dannenberg; S. Dapprich; A. D. Daniels; O. Farkas, J. B. Foresman; J. V. Ortiz; J. Cioslowski and D. J. Fox, Gaussian 09, revision C.01, Gaussian, Inc.: Wallingford, CT, 2009.
15. F. Yakuphanoglu, Ph.D. Thesis, Firat University, Elazig, Turkey (2002).
16. M. S. Massoud, S. A. El-Enein and E. El-Sherafy, *J. Therm. Anal.*, 37 (1991) 365.
17. G. V. Avramenko and B. I. Stepanov. *Zh. ObshchKhim.*, 44 (1974) 1298.
18. V. Bertolassi, V. Ferretti, P. Gilli, G. Gilli, Y. M. Issa and O. E. Sherif, *J. Chem. Soc. Perkin. Trans.*, 2 (1993) 2223.
19. V. Bertolassi, L. Nanni, P. Gilli, V. Ferreti, Y. M Issa and O. E. Sherif, *New J. Chem.*, 18 (1994) 251.
20. F. U. Z. Chowdhury and A. H. Bhuiyan, *Thin Solid Films*, 370 (2000) 78.
21. S. I. Shihub and R. D. Gould, *Thin Solid Films*, 254 (1995) 187.
22. M. R. Anantharaman, S. Sindhu, S. Jagatheesan, K. A. Molini and P. Kurian, *J. Phys D: Appl . Phys.*, 32 (1999) 1801.
23. A. R. Long, *Adv. Phys.*, 31 (1982) 553.
24. S. R. Elliot, *Adv. Phys.*, 36 (1987) 135.
25. K. Jonsher, *Dielectric Relaxation in Solids*, Chelsea Dietectiric Press, London, (1983).
26. S. R. Elliot, *Phil. Mag.*, 36 (1977) 1291.
27. S. Hazara and A. Ghosh, *Phil. Mag.*, B74 (1996) 235.
28. M. M. El-Nahass, H. M. Zeyada, M. M. El-Samanoudy and E. M. El-Menyawy, *J. phys. Condens. Matter.*, 18 (2006) 5163.

29. F. Yakuphanoglu, Y. Aydogdu, U. Schatzschneider and E. Rentschler, *Solid State Commun.*, 128 (2003) 63.
30. G. Austin and N. F. Mott., *Adv. Phys.*, 18 (1969) 41.
31. M. Pollak, *Phil. Mag.*, 23 (1971) 519.
32. M. Pollak and G. E. Pike. *Phys. Rev. Lett.*, 28 (1972) 1449.
33. G. E. Pike, *Phys. Rev.*, B6 (1972) 1572.
34. S. R. Elliot, *Phys. Mag.*, 37 (1978) 53.
35. M. M. Mosaad, A. El-Shawarby, Z. H. El-Tanahy and M. M. Abdel-Kader, *J. Mat. Sci.,: Materials in Electronics*, 6 (1995) 235.
36. M. M. Abdelkader, A. I. Aboud and W. M. Gamal, *Phase Transitions*, 88 (5) (2015), 445.